

ChemComm

Accepted Manuscript



This is an *Accepted Manuscript*, which has been through the Royal Society of Chemistry peer review process and has been accepted for publication.

Accepted Manuscripts are published online shortly after acceptance, before technical editing, formatting and proof reading. Using this free service, authors can make their results available to the community, in citable form, before we publish the edited article. We will replace this *Accepted Manuscript* with the edited and formatted *Advance Article* as soon as it is available.

You can find more information about *Accepted Manuscripts* in the [Information for Authors](#).

Please note that technical editing may introduce minor changes to the text and/or graphics, which may alter content. The journal's standard [Terms & Conditions](#) and the [Ethical guidelines](#) still apply. In no event shall the Royal Society of Chemistry be held responsible for any errors or omissions in this *Accepted Manuscript* or any consequences arising from the use of any information it contains.

Cite this: DOI: 10.1039/c0xx00000x

www.rsc.org/xxxxxx

ARTICLE TYPE

A highly stable face-extended diamondoid cluster-organic framework incorporating infinite inorganic guests

Wei-Hui Fang,^a Lei Zhang,^a Jian Zhang,^a and Guo-Yu Yang^{*a,b}

Received (in XXX, XXX) Xth XXXXXXXXX 20XX, Accepted Xth XXXXXXXXX 20XX

DOI: 10.1039/b000000x

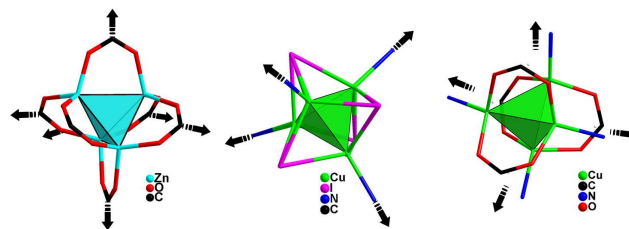
A highly stable face-extended cluster-organic framework incorporating infinite inorganic guests is hydrothermally made, in which the tetrahedral O-centred Cu₄O cluster is firstly found as the face-extended structure building unit to further make diamondoid cluster-organic framework with high thermal and structural stability.

The metal-organic frameworks (MOFs) have a history of nearly two decades from their origins to the present day.¹ As the term suggests, MOFs are porous crystalline solids assembled by inorganic structural building units (nodes) with organic ligands (linkers). Their architectures can be tailored with rational design methodology, not only allowing the customization of materials to yield desired physical and chemical properties,²⁻³ but also forming cationic, neutral and anionic MOFs. Generally, the guests are isolated inorganic anions in cationic MOFs,⁴⁻⁶ while the infinite anionic chain guests in cationic MOFs is rare and unprecedented. Despite the organic linkers can be amenably controlled in the synthesis of new MOFs, the formation of the inorganic nodes still seems "wild" to us. Till now, the most frequently used highly symmetrical inorganic nodes include the paddle-wheel,⁷ the triangle cornerstone shape cluster,⁸ the tetrahedron,⁹ and the octahedron,¹⁰ etc.

To a tetrahedron, there are four vertices, six edges and four faces. Theoretically, the tetrahedron can be extended via three ways: vertices, edges and faces. Of which the edge-extended linkage has firstly been observed in MOF-5 in 1999⁹ and well demonstrated in IRMOF-1-16.² Six carboxylates ride on six edges of tetrahedral Zn₄O cluster to form an octahedral six-connected Zn₄O(CO₂)₆ node (Scheme 1) in MOF-5. Apart from six edges, if tetrahedral cluster units are extended by vertices and faces, 4-connected zeolite-like frameworks will be constructed. Recently, a vertex-extended linkage of Cu₄I₄ cluster leads to the formation of a MTN-type zeolitic cluster-organic framework (COZ-1).¹¹ However, it still remains a great challenge to make cluster-organic frameworks *via* the face-extended linkages.

Our efforts focus on the design and synthesis of cluster-organic frameworks.¹²⁻¹⁴ Here, we report a highly stable cluster-organic framework based on tetrahedral O-centred Cu₄O clusters, [Cu₄(μ₄-O)L₄][Cu₄Br₈] (**1**, HL = 4-pyridin-4-yl-benzoic acid), in which the face-extended tetrahedral Cu₄O cluster is successfully realized and further connects each other to form a 4-connected diamondoid 3-D cluster-organic framework. In the tetrahedral Cu₄O cluster, three Cu atoms located on each triangle face

are fixed by one pyridyl nitrogen (N_{PY}) and two carboxylate oxygen (O_{COO}) atoms from two L ligands with reverse orientations (Scheme 1, right). Interestingly, the 1-D rhombic channels of the host framework are filled by the shape-matching inorganic chain guests.



Scheme 1 Scheme representation of the edge (left), vertex (middle) and face (right) expansion strategies of the tetrahedron building units in MOF-5, COZ-1 and this work, respectively.

Single-crystal structure determinations reveal **1** crystallizes in orthorhombic space group *Fddd*. The asymmetric unit of **1** consists of a cationic inorganic-organic hybrid host motif and an inorganic guest (Fig. S1). All Cu atoms are four-coordinated. The coordination environment of Cu atom in host motif is completed by one μ₄-O, two O_{COO} and one N_{PY}, and Cu atoms in guest motif are tetrahedrally bridged by four Br atoms. The bond lengths of Cu-O [1.943(5)-1.968(1) Å], Cu-N [1.972(6) Å], Cu-Br [2.478(2)-3.161(1) Å] are comparable to the related Cu complexes.^{7,15}

In the host motif, four equivalent Cu atoms define a tetrahedral Cu₄O cluster, in which a μ₄-O atom locates in the center (Fig. S2). Such O-centred cluster is reminiscent of familiar Zn₄O tetrahedron in MOF-5,⁹ in which six edges of the Zn₄O cluster are occupied by six carboxylates of 1,4-benzenedicarboxylate, resulting in a cubic net. While the Cu₄O clusters herein are linked by L ligands in μ₃-tridentate mode, producing a 4-connected *dia* cluster-organic framework. Although the isolated Cu₄O clusters have been well investigated,¹⁶⁻¹⁸ the extended structures built by tetrahedral Cu₄O clusters have never been documented. As shown in Fig. 1a, each pair of parallel L ligands has reverse orientations and connects two faces of adjacent tetrahedral Cu₄O clusters. And ten such Cu₄O clusters are linked each other *via* twelve pairs of L ligands into a very large adamantane cage with an edge length of 14.3 Å (Fig. 1b). Such face-extended linkage is unprecedented and completely differs from that of the vertex-/edge-extended linkages of the tetrahedral clusters.^{2,9,11} Due to the spacious nature of a single network, the overall framework of **1** exhibits a three-fold interpenetration (Fig. 1c, S3). The interpenetration vector

runs along the *a*-axis with a separated distance from one net to another of 8.0 Å (Fig. S4). Despite the existence of interpenetration, the framework is still open (porosity 31.0%¹⁹) and exists rhombic channels (cross-section $14.3 \times 14.3 \text{ \AA}^2$) along the *a*-axis. Also it represents the minimum number of interpenetrating *dia* net linked by L ligands till now (Table S1).²⁰⁻²⁶ The decrease of interpenetration degree may be attributed to the size increase of the inorganic nodes.

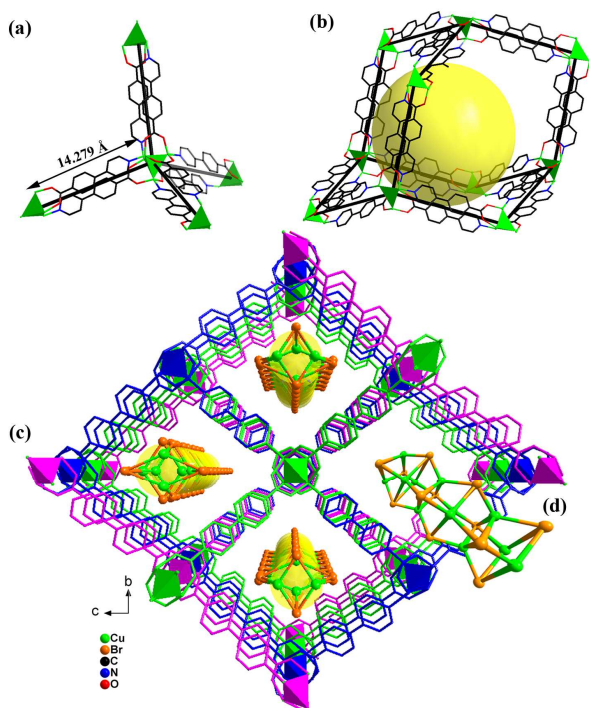


Fig. 1 The structure of **1**. (a) The coordination environment of the tetrahedral Cu_4O cluster; (b) The large adamantane unit; (c) The overall perspective view, in which the single network show different colors for clarity. (d) The ball-stick view of the infinite inorganic guest.

In guest motif, four Cu(2~5) atoms are all on crystallographic C_2 sites with half-occupied and bridged by Br atoms to form a chain: of which Cu(2) and Cu(3) centers are bridged by μ -Br to form a well-known $[\text{Cu}_2\text{Br}_6]^{4-}$ dimer motif,²⁷ which are further linked into chains by two μ -Br bridges and one additional copper atom (Cu(4) or Cu(5) atom) between each dicopper unit. However, the distance of Cu(4)...Cu(5) on their C_2 -symmetric lattice sites is 2.5 Å that is much too short to be real. Hence, only Cu(4) or Cu(5) can be occupied in each asymmetric unit, probably with a random distribution down each chain (Fig. 1d), which results in a Cu_3Br_4 unit. The Cu : Br ratio obtained from electron probe microanalysis agrees with this assignment. Such Cu_3Br_4 units further link each other to form 1-D Cu-Br chain based $[\text{Cu}_2\text{Br}_6]^{4-}$ dimers and $[\text{CuBr}_4]^{3-}$ tetrahedra.

The bond valence sum (BVS) shows the value of Cu(1) atom in Cu_4O motif is 1.81, and the values of Cu(2~5) atoms in Cu_3Br_4 motif are 0.95, 0.96, 0.94 and 0.97, indicating that the valences for Cu(1~5) atoms are 2, 1, 1, 1, 1, respectively (Table S2).

The most striking structural feature of **1** is the shape-matching combination of hybrid host framework and inorganic chain-like guests (Fig. 1c, S5). The rhombic channel around the guests matches the shape of the chain-like guest, which is unique and

different from that of known porous MOFs templated by amines.²⁸ In the structure, the infinite inorganic guests interact with the hybrid host framework via C-H...Br hydrogen bonding interactions (Fig. S6, Table S3).

In addition to the structural novelty, **1** also shows high thermal and water stability. The thermogravimetric analysis carried out in air atmosphere from 30 to 1000 °C showed one onset weight loss. **1** does not decompose until 400°C, which indicates the high thermal stability of its 3D cluster-organic framework (Fig. S7). In comparison with MOF-5 that is sensitive to moisture and water,⁴² the semiconductive (band gap = 2.32 eV, Fig. S8) crystalline samples of **1** exhibit highly stability. Its structure can be retained even after being exposed in air or soaked in water for months (Fig. S9).

To reveal the flexibility between the host and guest motifs, the thermal expansion properties of **1** were studied. From 100 to 500 K, the unit-cell parameters show approximately linear changes and the unit-cell volume expand about 2.6% (Fig. 2, Table S4). The thermal expansion coefficients of *a* and *b*-axis are $49 \times 10^{-6} \text{ K}^{-1}$ and $65 \times 10^{-6} \text{ K}^{-1}$, respectively, which are in agreement with the thermal expansion law. However, the length of *c*-axis ($-49 \times 10^{-6} \text{ K}^{-1}$) reduces when increasing temperatures, resulting in a negative thermal expansion coefficient of $-49 \times 10^{-6} \text{ K}^{-1}$. In order to analyze the structural origin of the thermal expansion of **1**, its single-crystal structures measured at 100 K and 298 K were compared (Table S5) and found that the changes were small in coordination bond lengths ($< 0.026 \text{ \AA}$) but large in the angles (max = 1.3°) (Table S6). Consequently, the 4-connected Cu_4O “rhombus grid” was distorted (Fig. S10), with two interior angles change approximately 1.1° and 0.5°. The positive/negative thermal expansion coefficients of **1** are not significant compared with typical thermal expansion materials,³⁰⁻³¹ indicating that the expansion of the host framework is restricted by the inorganic guests.

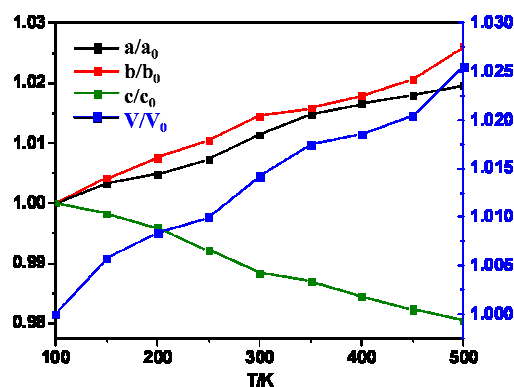


Fig. 2 Relative changes in the lattice parameters *a*, *b*, *c* and volume of **1** (normalized to their values at 100 K) vs temperature.

In view of the robust architecture of **1**, TEM images were studied to visualize its pores as those reported for IRMOF-74-VII and IRMOF-74-IX.⁴⁵ However, the attempts to observe the arrangement of the channels of **1** were unsuccessful due to its sensitivity to the electron beam. Instead, spherical and uniform nanoparticles (NPs, $< 5 \text{ nm}$) are found (Fig. 3a). Fast Fourier transform (FFT) analysis was performed on the centered square areas in the HRTEM images (Fig. 3b). Six reflection spots

corresponding to the 110 reflections were resolved from the FFT patterns. The interlayer distance of the selected area is calculated to be 0.201 nm, which agrees well with the (110) lattice planes of hexagonal phase CuBr (PDF#06-0700). Considering the compositions of the Cu₃Br₄-based chains in **1**, it is reasonable to conclude that the formation of these CuBr NPs should be attributed to the decomposition and rearrangement of these Cu₃Br₄-based chains.

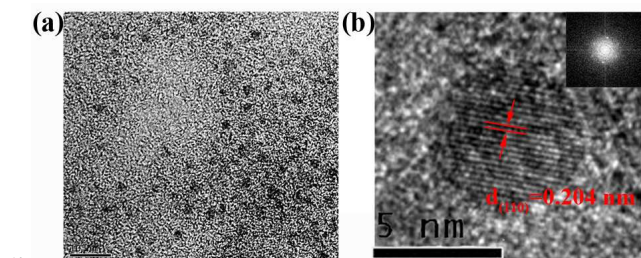


Fig. 3 (a) TEM micrographs of the NPs of **1**. Scale bar 10 nm. (b) HRTEM image of an individual particle. Inset is the FFT pattern.

In summary, a highly stable face-extended cluster organic framework incorporating infinite inorganic chains has been successfully made under hydrothermal conditions. The key points of the synthetic procedures have been well established. It represents a rare example in the face-extended linkages, which makes it different from other cluster organic frameworks with vertex-/edge-extended linkages. This study may open up possibilities for making novel frameworks constructed from the face-extended cluster building units. Further work is in progress.

This work was supported by the NSFC (nos. 21401191, 91122028, and 21571016), the 973 Program (nos. 2014CB932501), and the NSFC for Distinguished Young Scholars (no. 20725101).

Notes and references

^aState Key Laboratory of Structural Chemistry, Fujian Institute of Research on the Structure of Matter, Chinese Academy of Sciences, Fuzhou, Fujian 350002, China. E-mail: ygy@fjirm.ac.cn ^bMOE Key Laboratory of Cluster Science, School of Chemistry, Beijing Institute of Technology, Beijing 100081, China. E-mail: ygy@bit.edu.cn

† Electronic Supplementary Information (ESI) available: X-Ray structure data in CIF files for compound **1**; Materials and physical measurements; IR spectra; TGA curves; PXRD patterns; Table S1-S6. CCDC 1051665.

‡ Synthesis of [Cu^{II}₄(μ₄-O)L₄][Cu^I₆Br₈] (**1**): A mixture of Gd₂O₃ (0.25 mmol, 0.091 g), CuBr (0.30 mmol, 0.043 g) and HL (0.50 mmol, 0.099 g) was added to a mixed solution of pivalic acid (0.202 g, 2.00 mmol) and water (5ml). After stirring for half an hour, the mixture was sealed in a 20 ml vial and transferred into a preheated oven at 180°C for 13 days, and then cooled to room temperature. The orange single crystals of **1** were washed with water and ethanol, and dried at room temperature (Yield: 40%). Elem Anal. Calcd. for C₄₈H₃₂Br₈Cu₁₀N₄O₉: C 27.67, H 1.55, N 2.69. Found: C 28.45, H 1.59, N 2.66. The phase purity of **1** has also been confirmed by powder X-ray diffraction (Fig. S11).

§ Crystal data for **1**: C₄₈H₃₂Br₈Cu₁₀N₄O₉, *M* = 2083.46, orthorhombic, *a* = 7.9878(1) Å, *b* = 33.9352(6) Å, *c* = 39.1992(7) Å, *V* = 10625.6(3) Å³, *T* = 100(2) K, space group *Fddd*, *Z* = 8. 9896 reflections measured, 2692 independent reflections (*R*_{int} = 0.0227). The final *R*₁ values were 0.0606 (*I* > 2σ(*I*)). The final *wR*(*F*²) values were 0.1881 (*I* > 2σ(*I*)). The final *R*₁ values were 0.0616 (all data). The final *wR*(*F*²) values was 0.1884 (all data). The goodness of fit on *F*² was 1.166.

1. O. M. Yaghi, G. M. Li and H. L. Li, *Nature*, 1995, **378**, 703.

- M. Eddaoudi, J. Kim, N. Rosi, D. Vodak, J. Wachter, M. O'Keeffe and O. M. Yaghi, *Science*, 2002, **295**, 469.
- Y. B. Zhang, W. X. Zhang, F. Y. Feng, J. P. Zhang and X. M. Chen, *Angew. Chem., Int. Ed.*, 2009, **48**, 5287.
- H.-R. Fu, Z.-X. Xu and J. Zhang, *Chem. Mater.*, 2015, **27**, 205.
- X. Li, H. Xu, F. Kong and R. Wang, *Angew. Chem., Int. Ed.*, 2013, **52**, 13769.
- X. Zhao, X. Bu, T. Wu, S. T. Zheng, L. Wang and P. Feng, *Nat. Commun.*, 2013, **4**, 2344.
- S. S. Chui, *Science*, 1999, **283**, 1148.
- G. Ferey, C. Mellot-Draznieks, C. Serre, F. Millange, J. Dutour, S. Surble and I. Margiolaki, *Science*, 2005, **309**, 2040.
- H. Li, M. Eddaoudi, M. O'Keeffe and O. M. Yaghi, *Nature*, 1999, **402**, 276.
- J. H. Cavka, S. Jakobsen, U. Olsbye, N. Guillou, C. Lamberti, S. Bordiga and K. P. Lillerud, *J. Am. Chem. Soc.*, 2008, **130**, 13850.
- Y. Kang, F. Wang, J. Zhang and X. Bu, *J. Am. Chem. Soc.*, 2012, **134**, 17881.
- S. T. Zheng, J. Zhang and G. Y. Yang, *Angew. Chem., Int. Ed.*, 2008, **47**, 3909.
- M. B. Zhang, J. Zhang, S. T. Zheng and G. Y. Yang, *Angew. Chem., Int. Ed.*, 2005, **44**, 1385.
- J. W. Cheng, J. Zhang, S. T. Zheng, M. B. Zhang and G. Y. Yang, *Angew. Chem., Int. Ed.*, 2006, **45**, 73.
- T. S. Lobana, R. Sultana and R. J. Butcher, *Dalton Trans.*, 2011, **40**, 11382.
- A. M. Kirillov, M. N. Kopylovich, M. V. Kirillova, M. Haukka, M. F. C. G. da Silva and A. J. L. Pombeiro, *Angew. Chem., Int. Ed.*, 2005, **44**, 4345.
- B. F. Abrahams, M. G. Haywood and R. Robson, *Chem. Commun.*, 2004, 938.
- A. Ozarowski, I. B. Szymanska, T. Muziol and J. Jezierska, *J. Am. Chem. Soc.*, 2009, **131**, 10279.
- A. L. Spek, *Acta Crystallogr., Sect. D: Biol. Crystallogr.*, 2009, **65**, 148.
- S. K. Elsaidi, M. H. Mohamed, L. Wojtas, A. Chanthapally, T. Pham, B. Space, J. J. Vittal and M. J. Zaworotko, *J. Am. Chem. Soc.*, 2014, **136**, 5072.
- Y. P. He, Y. X. Tan and J. Zhang, *CrystEngComm*, 2012, **14**, 6359.
- O. R. Evans and W. B. Lin, *Chem. Mater.*, 2001, **13**, 2705.
- T. B. Lu and R. L. Luck, *Inorg. Chim. Acta*, 2003, **351**, 345.
- X. J. Zhou, B. Y. Li, G. H. Li, Q. Zhou, Z. Shi and S. H. Feng, *CrystEngComm*, 2012, **14**, 4664.
- G. Mehlana, G. Ramon and S. A. Bourne, *CrystEngComm*, 2013, **15**, 9521.
- M.-H. Zeng, Y.-X. Tan, Y.-P. He, Z. Yin, Q. Chen and M. Kurmoo, *Inorg. Chem.*, 2013, **52**, 2353.
- J. Beck and A. Bof de Oliveira, *Z. Anorg. Allg. Chem.*, 2009, **635**, 445.
- Q. R. Fang, G. S. Zhu, Z. Jin, Y. Y. Ji, J. W. Ye, M. Xue, H. Yang, Y. Wang and S. L. Qiu, *Angew. Chem., Int. Ed.*, 2007, **46**, 6638.
- S. Hausdorf, J. Wagler, R. Mossig and F. O. R. L. Mertens, *J. Phys. Chem. A*, 2008, **112**, 7567.
- A. L. Goodwin, M. Calleja, M. J. Conterio, M. T. Dove, J. S. O. Evans, D. A. Keen, L. Peters and M. G. Tucker, *Science*, 2008, **319**, 794.
- H. Zhou, M. Li, D. Li, J. Zhang and X. Chen, *Sci. China Chem.*, 2014, **57**, 365.
- H. Deng, S. Grunder, K. E. Cordova, C. Valente, H. Furukawa, M. Hmadeh, F. Gandara, A. C. Whalley, Z. Liu, S. Asahina, H. Kazumori, M. O'Keeffe, O. Terasaki, J. F. Stoddart and O. M. Yaghi, *Science*, 2012, **336**, 1018.